

Giant Gain Enhancement in Photonic Crystals with a Degenerate Band Edge

Mohamed A. K. Othman¹, Farshad Yazdi¹, Alex Figotin² and Filippo Capolino¹

¹*Department of Electrical Engineering and Computer Science, University of California, Irvine, Irvine, CA, USA. 92697*

²*Department of Mathematics, University of California, Irvine, Irvine, CA, USA 92697.*

{mothman, fyazdi, afigotin, f.capolino}@uci.edu

Cavities made of photonic crystals incorporating active material have already demonstrated a stronger gain enhancement when operating at the regular band edge (RBE) of a dispersion diagram. Here instead we propose a new idea that leads to giant gain enhancement based on utilizing the unconventional slow wave resonance associated to a degenerate band edge (DBE) in the dispersion diagram of photonic crystals. We show that the gain enhancement in a Fabry-Perot cavity when operating at the DBE is several orders of magnitude stronger when compared to a cavity of the same length made of a photonic crystal with RBE. We also have found critical conditions for maximizing the total power gain. The giant gain is explained by significant increase in the photon lifetime and the local density of states. We have demonstrated DBE operated cavities that provide for superior gain conditions for lasers, quantum cascade lasers, traveling wave tubes, and distributed amplifiers with solid state.

I. INTRODUCTION

Light confinement using either mirrors or Bragg reflectors can form high quality (Q)-factor Fabry-Perot cavity (FPC) resonators with enhanced optical field intensity. Such cavities are typically used for laser applications and spectroscopy. An important class of high Q -factor structures is formed by slow-wave resonators based on the regular band edge (RBE) of the wavenumber-frequency dispersion diagram relative to photonic crystals, whose simplest architecture is a periodic stack of dielectric layers, with one dimensional periodicity [1–3]. More elaborate designs of nanocavities adopted Silicon heterostructures [4], liquid crystals [5] technologies and demonstrated improvement in the Q -factor compared to previously reported designs. The use of photonic crystals resulted in enhanced amplification properties for low-threshold lasing [2], coherent quantum electron–photon interactions [6], nonlinear optics [7] and quantum processing [8].

As proposed by Figotin and Vitebsky in [9–13], FPC resonators made of photonic crystals composed by anisotropic dielectric layers can exhibit sharp transmission peaks very close to the photonic band

edge frequency. Many interesting field enhancement properties are also manifested, due to degeneracy condition of the structural eigenvalues, namely the degenerate band edge (DBE) condition. We demonstrate in this paper that based on the resonance properties discussed in [9–13], the DBE condition leads to giant power gain when active material is incorporated in a periodic structure. The power gain obtained can be several orders of magnitude stronger than that obtained by a comparable photonic crystal with RBE. In both cases slow-light is involved, but we demonstrate here that the DBE condition is far superior to the RBE condition for enhancing the power gain. An example of giant gain in a periodic DBE structure is clearly shown by the peak in Fig. 1 (red curve). This periodic structure is made of three layers, two anisotropic and one isotropic, exhibiting a DBE as those in [10–12], amplification occurs when incorporating active material. The layered stack with three different colors in the inset of Fig. 1 shows the DBE-based structure. The method used to calculate the transmission power gain is detailed in section III. The layer that includes active material, and thus intrinsic gain, is isotropic and it can be realized by either layers of quantum wells, Raman scattering

mechanisms or layers doped with active materials like Erbium, for example. A possible implementation of the anisotropic layers can be carried out utilizing liquid crystals, for instance, that can possess tunable anisotropic properties [5,14]. We would like to point out that the conceptual findings reported in this paper not only apply to stacks of anisotropic layers, but also to various other periodic guiding structures that exhibit the DBE condition, such as optical coupled waveguides/nanowires systems made with silicon-on-insulator technology embedded with gratings, as those in [15–17] for example. An attractive application for such amplification scheme is quantum cascade lasers, superior to the one obtained using isotropic type of photonic crystals as in [18], with the promise of very high quantum efficiency.

II. BACKGROUND AND METHODS

The goal of this paper is to show a possibility of giant amplification in a gain medium, that to our best knowledge have not been observed before. Such a gain medium is provided by a periodic structure supporting a DBE as we demonstrate for a specific example based on ideas expressed first in [19]. To understand origins of the giant gain let us recall some basic properties of DBE in photonic crystals. With reference to Fig. 2(a-b) and to [9–13], we show the dispersion diagram (that relates frequency to the complex Bloch wavenumber k) for modes associated with a specific periodic structure used in our demonstrations. (Note that in [9-13] only the real part of these Bloch wavenumbers was shown). The Bloch modes may exhibit an RBE condition at a certain frequency ω_g . When two or more modes are allowed to propagate at the same frequency a crystal may also exhibit a DBE at a frequency ω_d or the split band edge (SBE) conditions. Waves with (k, ω) in the vicinity of those stationary points of the dispersion diagram exhibit almost vanishing group velocity; a consequence of multiple reflections. These waves experience an effective increase in the optical path. Indeed, the increase in group index at an RBE condition was the basis for various studies suggesting

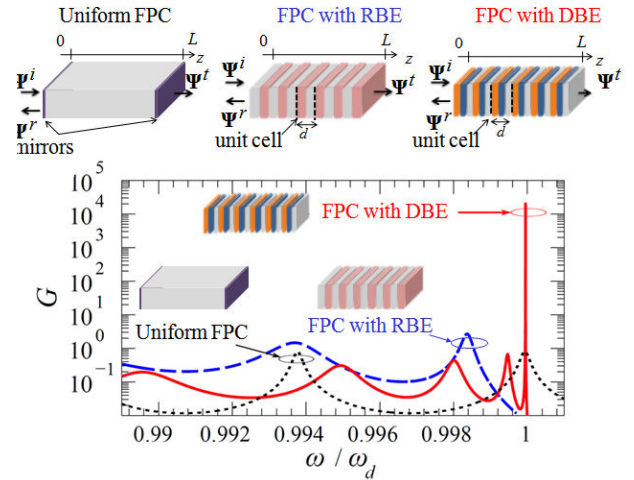


FIG. 1. Total transmission power gain G for three cavities: uniform FPC (dotted), FPCs formed by a periodic structures that exhibit either an RBE made of isotropic layers (dashed) or a DBE made of misaligned anisotropic (birefringent) layers (solid) at ω_d . In the top geometries, the unit cell boundaries are marked by dashed black lines. Active material is embedded in only the isotropic (gray) layers, having $n'' = -2.2 \times 10^{-4}$.

possible gain enhancement in FPCs with RBE (see, for example, [20,21] and references therein). The wavenumber-frequency dispersion relation for the propagating mode can be approximated by the asymptotic expression $\Delta\omega \propto (\Delta k)^2$ near an RBE and by $\Delta\omega \propto (\Delta k)^4$ near a DBE, where the increments are with respect to the stationary condition. We will show that this implies a gigantic increase in the density of states (electromagnetic modes) and the group index near a DBE compared to what happens near an RBE. In turn, this implies resonators Q -factors that are orders of magnitude higher than their RBE counter parts [22] that scale as $Q \sim N^5$ [10], with N being the number of unit cells of the dielectric stack. The Q -factor improvement in FPCs with DBE can be understood by observing a larger amount of average electromagnetic energy stored inside the resonator, compared to the energy leaking outside (when dissipation due to material losses is negligible compared to the power leaking out). In other words, the cavity effective mode volume [23] shrinks significantly close to a DBE condition, leading to

high levels of field enhancement. In section III, we will relate the enhancement of the Q -factor to the giant gain through concept of photon lifetime. Such intriguing features of DBE structures are investigated here are considered as a recipe for gigantic boost in power gain, in addition to efficient manipulation of the lifetime of quantum emitters, the Purcell factors as well as nonlinear effects in DBE-based structures.

III. GIANT GAIN AND THE WIGNER TIME INCREASE

We show in this section that the gain in an FPC operated at DBE is enhanced by several orders compared to one with an RBE condition (Fig. 1). This giant gain enhancement can be explained by a significant increase of the Wigner time compared to that for other cavities. To see that let us consider three kinds of FPCs. The first one is a conventional FPC formed by an isotropic and homogenous dielectric material bounded by two highly reflective mirrors, referred to as uniform FPC, as shown in Fig. 1. The second one is made by stacking isotropic dielectric bi-layers (referred to as FPC with RBE and shown in Fig. 1). The third one is made by stacking anisotropic tri-layers (referred to FPC with DBE) as depicted in Fig. 1, with two anisotropic layers of the same thickness $0.31d$, and an isotropic one of thickness $0.38d$, with parameters given in Appendix A. The two periodic structures have the same unit cell thickness d , and the FPC length is $L = Nd$. We assume that the FPC with RBE is constructed from alternating dielectric layers with $n_1 = 3.2$ and $n_2 = 1.5$ with equal thickness designed to have a band edge at $\omega_g = \omega_d$ for the sake of comparison, while the uniform FPC has a refractive index of $n = 2.25$. Note that the selection of boundaries for the unit cell is depicted in the inset of Fig. 1 by dashed lines. Inside the anisotropic layers, the x and y polarizations are coupled therefore we elaborate on the electromagnetic field representation inside those layers. The guided time-harmonic electromagnetic fields (varying as $e^{-i\omega t}$) along the z -direction associated to these *two* coupled waves are described

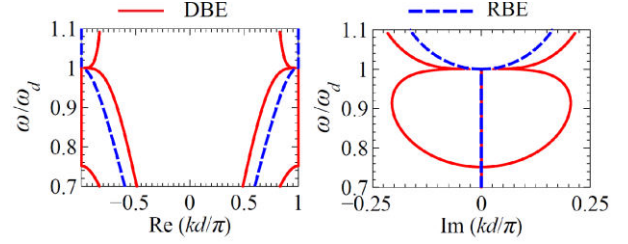


FIG. 2. Dispersion relations $k-\omega$, showing the real and imaginary parts of the Bloch wavenumber for the two periodic structures in the inset of Fig. 1: one that exhibits only RBE at ω_d . (dashed) and another that exhibits DBE at ω_d (solid).

by a *four* dimensional state vector $\Psi(z) = [E_x \ E_y \ H_x \ H_y]^T$, which satisfies Maxwell's equations and boundary conditions at the interfaces between layers, and evolves along the z -direction [10,12]. The transformation across a unit cell of length d is described by using a 4×4 transfer matrix $\underline{\mathbf{T}}(z+d, z)$ that relates the field between two points z and $z+d$ as $\Psi(z+d) = \underline{\mathbf{T}}(z+d, z)\Psi(z)$. Such transfer matrix is found by cascading the transfer matrices of the constitutive layers $\underline{\mathbf{T}}_m$ as
$$\underline{\mathbf{T}}(z+d, z) = \prod_{m=1}^M \underline{\mathbf{T}}_m$$
, with M being the number of layers per unit cell (for example $M = 3$ for the DBE structure analyzed here, and $M = 2$ for the RBE structure), and $\underline{\mathbf{T}}_m = \underline{\mathbf{T}}_m(z+d_m, z+d_{m-1})$ where d_m is the thickness of the m th layer, and $d_0 = 0$. Details of calculation of such transfer matrix are presented in Appendix A. By solving the eigensystem $\underline{\mathbf{T}}(z+d, z)\Psi(z) = \lambda\Psi(z)$, one obtains the eigenvalues λ related to the Bloch wavenumber k as $\lambda = e^{ikd}$ that defines the modal propagation. The DBE condition is equivalent to the requirement for $\underline{\mathbf{T}}(z+d, z)$ to be similar to a Jordan block [10,11].

The Brillouin zone dispersion relation for the periodic structures whose unit cell defines the periodic type of FPCs is depicted in Fig. 2, showing the real and imaginary parts of the eigenmode Bloch wavenumber k . For symmetry reasons, both k and $-k$ are modal

solutions. Accordingly, the photonic crystal with pairs of isotropic layers supports only one propagating mode in the each direction below the RBE (for instance at $\omega = 0.75\omega_g$ with $\omega_g = \omega_d$). Instead, the structure with anisotropic layers is able to support two modes simultaneously propagating in the each direction below the RBE (for instance at $\omega = 0.75\omega_d$) and only one propagating mode (the other is evanescent) below the DBE at $\omega = \omega_d$. Just below ω_d , there exists only one propagating mode for the RBE and DBE cases, as seen in Fig. 2. This propagating mode in the $+z$ -direction (pertaining to the $+k$ solution in the unbounded periodic structure) has a unique state vector denoted by Ψ_1 , whose electric field components are described by the vector $\mathbf{E}_1 = [E_{x1} \quad E_{y1}]^T$.

For a finite stack of N unit cells as in the inset of Fig. 1 we report the exact total transmission power gain in Fig. 1 calculated as $G = P_{\text{out}} / P_{\text{inc}}$ where P_{inc} and P_{out} are the time-average incident and transmitted power densities, respectively. We consider a transverse electromagnetic (TEM) plane wave excitation with an electric field vector \mathbf{E}^i that is polarized along the vector \mathbf{E}_1 . The electric fields transmitted through the FPC comprise a vector \mathbf{E}^t , and the incident and transmitted power densities are calculated as $\frac{1}{2}\|\mathbf{E}^i\|^2/\eta$ and $\frac{1}{2}\|\mathbf{E}^t\|^2/\eta$, respectively, with η being the wave impedance of the surrounding material, assumed to be vacuum, and $\|\cdot\|$ represents the norm of the vector. In this example we take $n'' = -2.2 \times 10^{-4}$ describing the isotropic active material with intrinsic gain, represented by the grey layers in the geometries in Fig. 1. For the DBE case the active layer is only in the isotropic region. Therefore the active material filling factor f is 100% for the uniform FPC, $f = 50\%$ for the FPC with an RBE, and $f = 38\%$ for the FPC with a DBE (38% is the filling factor of the isotropic layers in the FPC

with DBE as explained in Appendix A), and both FPCs have $N=32$ unit cells. Despite the smallest active filling fraction, the structure with DBE is the one that provides giant amplification, up to four orders of magnitude larger than the FPC with RBE, as shown in Fig. 1 where we compare the total amplification provided by the structure with an RBE structure and a uniform FPC. The reasons for such giant enhancement in gain is quantified in the following section.

A. Transmission characteristics

We calculate here the transmission coefficient T for the same stack of N unit cells shown in Fig.1. This coefficient is polarization dependent on the impinging TEM plane wave due to the anisotropy of some layers in the FPC with DBE. We select the same incident polarization used to calculate the gain in Fig. 1., i.e., matched to the polarization state \mathbf{E}^i of the mode supported by the infinite structure. We define the transmission coefficient for FPC of length L as the projection of the transmitted electric field vector \mathbf{E}^t on \mathbf{E}^i , i.e., $T = \langle \mathbf{E}^t, \mathbf{E}^i \rangle / \|\mathbf{E}^i\|$ where the brackets denote the inner product of those two vectors in complex normed space, with $\|\mathbf{E}^i\|$ as the norm. We observe in Fig. 3(a) a very narrow (high Q -factor) transmission peak for the FPC with a DBE, with $N = 32$ unit cells. This occurs at an angular frequency very close and lower than to the DBE angular frequency ω_d , because strong reflection occurs at ω_d and for higher frequencies due to an existing bandgap [10,11]. The transmitted spectrum is densely-packed with resonances, for the FPC with DBE near the DBE frequency. By neglecting the phase shift introduced by the interfaces, the wavenumber of the DBE resonance mode for large number of unit cells N is estimated by $k_{r,d} \approx \pi/d - \pi/(Nd)$, and the corresponding resonance frequency $\omega_{r,d}$ can be calculated as $\omega_{r,d} \approx \omega_d - \frac{b}{d^4} \left(\frac{\pi}{N} \right)^4$ as shown in

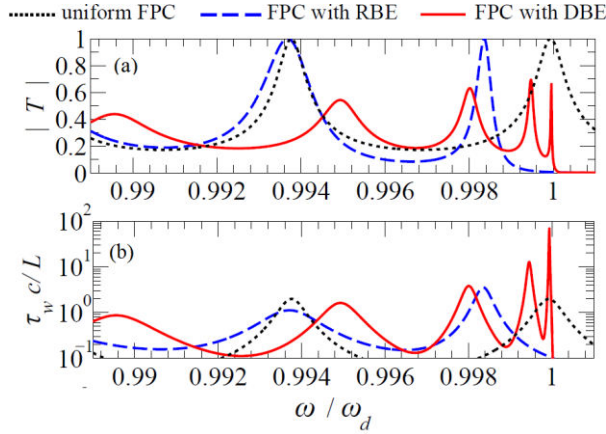


FIG. 3. (a) Magnitude of the transmission coefficient, (b) Wigner time for three types of FPCs: uniform FPC (dotted), FPCs formed by a periodic structures that exhibit either an RBE (dashed) or a DBE (solid) at ω_d .

Refs. [10,11] where b is a problem specific constant. For the RBE case we have a similar approximation of the resonance frequency, with $1/N^2$ instead of $1/N^4$ [3,20,24]. In addition, FPCs in Fig. 1, with RBE and DBE, respectively, exhibit a high quality factor resonance without using mirrors whereas the uniform FPC necessitates mirrors to reach the same quality factors of an RBE FPC cavity. Such mirrors, designed here with $\sim 95\%$ power reflectivity can be realized by, for example, large stacks of Bragg reflectors.

B. Wigner time and photon lifetime

Transmission properties considered in previous section are the first indicators of a possibility of enhancing gain in FPCs with a DBE. Estimation of the photon lifetime inside the FPC is yet another pass to origins of the gain enhancement. Before assessing the photon lifetime, we notice that the Wigner time of FPC (also referred to as tunneling time or group delay) is another important quantity that can be easily obtained for our structure. The Wigner time is defined as $\tau_w(\omega) = d\varphi(\omega)/d\omega$, where $\varphi(\omega)$ is the total transmission phase shift accumulated across the FPC of length L , i.e., the phase of the T coefficient. As explained in [25–27], this quantity is a measure of the effective group velocity of photons passing through the FPC. Fig. 3(b) shows the normalized Wigner time for the three FPCs under study, showing more than an order of magnitude increase for the FPC

with a DBE, near ω_d . The other two types of FPCs have similar Wigner time since the resonances of those have similar Q factor for the chosen cases. Although Wigner time calculated here is based on the phase of the transmission coefficient defined previously, we have observed (not shown here) that at the DBE τ_w becomes almost polarization independent owing to the rapid variation of the phase, $\varphi(\omega)$ at the DBE resonance.

The Wigner time is required to calculate the effective optical path length L_{eff} , that is the length required for photons to traverse the cavity, calculated as $L_{\text{eff}} = n_{\text{eff}}L$, where n_{eff} is the effective group index of the cavity. Accordingly, the effective group index is given as $n_{\text{eff}} = c\tau_w/L$ where c is the speed of light in vacuum, and τ_w is the Wigner time of the cavity before introducing materials with intrinsic gain. The effective length, $L_{\text{eff}} = c\tau_w$ dramatically increases near a DBE as a consequence of the Wigner time enhancement.

When active material, described by complex refractive index $n = n' + in''$ with $n'' < 0$, is included in the FPC, the photon *single pass* power gain coefficient the composite medium is given by $g_0 = \gamma Lf$, where f is the active material filling factor in the cavity and γ is the per-unit-length material intrinsic gain coefficient. The latter is related to the positive imaginary part of the material refractive index as $\gamma = -2k_0n''$ with k_0 being the wavenumber in vacuum. We define an effective gain coefficient g_{eff} as the gain experienced by photons traveling through the FP cavity, estimated as

$$g_{\text{eff}} = g_0 L_{\text{eff}} / L = g_0 n_{\text{eff}} = \gamma f c \tau_w. \quad (1)$$

This reveals that the effective gain coefficient of an FPC is the product of the intrinsic material gain coefficient and the FPC Wigner time. The above is valid under the assumption that γ is relatively small so as not to deteriorate the modal properties of the DBE resonance, as discussed in the following section. Notice also that the transmission power gain is in

general polarization dependent and there exists specific polarizations maximizing the gain. However, it is the Wigner time that plays the key role for the giant power gain enhancement, with far more significant impact on the power gain than the incident polarization. The total power gain G at a DBE resonance can be estimated using the effective gain coefficient, as follows. Let us denote G_{approx} as an estimate of the exact total power calculated as $G_{\text{approx}} = |T|^2 e^{\mathcal{G}_{\text{eff}}}$ at resonance. This is a simple way to approximate the small-signal amplifier transmission power gain from the transmission and gain coefficients. Note that the scaling with the transmission coefficient is necessary here to retrieve an estimate of total power transmission gain G_{approx} , since $|T| \neq 1$ at a DBE resonance as seen in Fig. 3. In section V we quantify and compare the estimation of the total power gain using such formula and the power gain shown in Fig. 1. We would like to point out that in general, for the purpose of constructing an effective gain coefficient, the separation of effects between cavity and material properties implied by (1), with τ_w and γf , respectively, cannot be established if the resonance is largely perturbed as discussed in the next section.

It is instructive to compare the Wigner time with the concept of photon lifetime τ_c , which is the time it takes the stored energy to decays to $1/e$ of its original value due to dissipation. Such quantity is frequently used in laser physics to express the resonator finesse [25–27] as well as to provide a good estimation of the Winger time, as explained in many different situations [24,28–32]. Although lifetime and group delay are different concepts, they are intimately related. Indeed, for a uniform lossless FPC at resonance we have an exact identity $\tau_c = \tau_w$ [30,32], which means that stored energy lifetime in such cavity identically equals to the time it takes the wave packet to traverse the whole FPC [32], but this identity is not exactly satisfied in general. The importance of τ_c relies in its explicit link to the Q -factor via $Q = \omega \tau_c$ [26,27], whereas there exist approximations of the Q factor using the Wigner time [29]. The lifetime quantifies the evolution of energy with time inside the FPC. Near the DBE, τ_c is extremely large because the quality factor is

enhanced [10,13] leading to eminently high levels of stored energy. This may have impacts on significantly lowering the lasing threshold condition in laser devices.

IV. CRITICAL GAIN CONDITION

Since DBE is a precise mathematical condition, i.e., it only emerges when the transfer matrix becomes similar to a Jordan Block, a large amount of extrinsic perturbation (active material with $n'' < 0$) can eventually deteriorate this condition. To put things into perspective, large single pass gain g_0 can deteriorate the slow-wave phenomena condition associated to the DBE implying that large enhancement of photon lifetime would not occur anymore. On the other hand usually very small single pass gain g_0 will not result in strong amplification [21]. Therefore, one may expect that there exist an optimum amount of active material filling, large enough to surpass losses in the FPC but small enough not to significantly perturb the DBE condition, hence resulting in maximized amplification. This is shown in Fig. 4 where we report the power transmission gain G varying the imaginary part of the refractive index n'' (which may be a result of tuning the pump power or volume concentration of active material). We observe a clear feature of such FPC, operating near the DBE, that makes clear the existence of an optimum amount of material gain to achieve the maximum amplification G . For instance for $N = 30$ unit cells the maximum

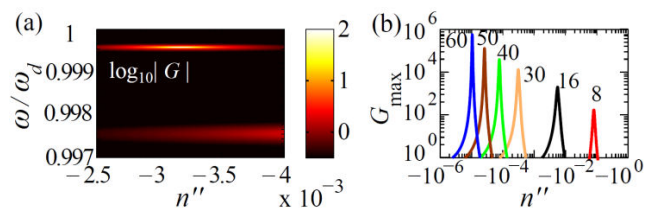


FIG. 4. (a) Plot of total power gain G varying as a function frequency and the material gain n'' around the DBE frequency for an FPC with DBE, with $N = 16$. (b) Maximum power gain G achieved and the optimum values of n'' , for different number of layers N indicated by the numbers.

power gain G_{\max} is 10^4 , relative to an optimum $n'' \cong -6 \times 10^{-4}$, whereas when $N = 50$ the maximum is 3×10^5 relative to an optimum $n'' \cong -5 \times 10^{-5}$. Therefore a careful selection of the intrinsic gain distribution inside the FPC may result in large amplification (due to better field enhancement and localization) with even less single pass intrinsic gain, leading to a higher power conversion efficiency in laser amplifiers. Note that for simplicity, gain

saturation effects and lasing line shapes are ignored in this study since we deal with a narrow band phenomenon whose bandwidth is in general much smaller than the laser line shape for homogenous broadening mechanisms. Furthermore, gain saturation that is a result of nonlinear effects is important when dealing with laser oscillators which will be subject of a future investigation, whereas in this premise we study small signal, linear giant amplification regimes.

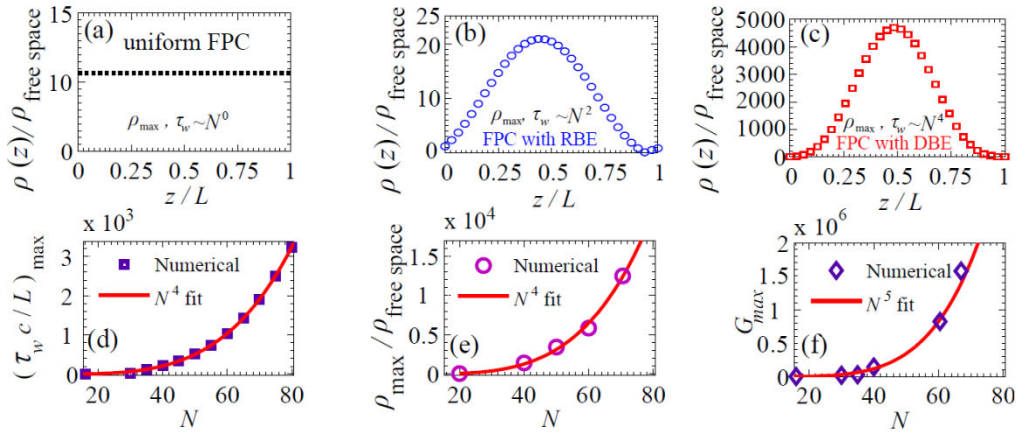


FIG. 5. Sampled local density of states (LDOS) normalized by the LDOS in free space inside (a) uniform FPC sampled at maxima locations, (b) FPC with RBE and (c) FPC with DBE sampled at points $z = md$, $m = 0, 1, 2, \dots, N$ with $N = 32$. (d-e) Trend of the Wigner time and LDOS varying the number of unit cells N showing an accurate fit to N^4 , and (f) is the trend of the maximum achievable power transmission gain fitted to N^5 .

V. GIANT ENHANCEMENT OF LOCAL DENSITY OF STATES

As a final step toward providing a comprehensive picture of the modal properties of an FPC with DBE that contribute to giant gain, we investigate the local density of states (LDOS) inside the FPC with DBE. Fermi's golden rule states that the emitters' decay rates are proportional to the LDOS in an open resonator [6,23]. We define the LDOS in an open, lossless FPC to be proportional to the imaginary part of the trace of the dyadic Green's function as [3,24,33]

$$\rho(z) = -2 \frac{k_0}{\pi c} \text{Im}(\text{Tr}[\underline{\mathbf{G}}(z, z)]), \quad (2)$$

where here Im and Tr denote imaginary part and trace, respectively. For the particular case where a DBE is present, we apply the transfer matrix formalism, analogously to what was done in [24,34,35] for a simpler photonic crystal, to retrieve the dyadic Green's function pertaining to a planar electric dipolar source, i.e., an electric source polarized along the x and y coordinates on a sheet at $z = \text{constant}$ (see Appendix B for calculation details). We report in Fig. 5(a-c) the LDOS normalized by the LDOS in free space for the three types of FPCs. For simplicity the LDOS is sampled once per unit cell in the two periodic structures since it varies within each unit cell. We observe that the LDOS for the FPC with DBE or with RBE peaks around the cavity center. Vice versa the uniform FPC has a uniform LDOS envelope

across the length (evaluated as sampling the LDOS at each maximum of the electric field) and the envelope is independent on the resonant mode; only the number of maxima depends on the chosen resonance.

Such enhancement in LDOS for the DBE case is due to the unconventional DBE resonance giant fields that exists inside the cavity. This giant field inside the cavity is generated thanks to a strong excitation of both propagating and evanescent modes in the FPC as a necessity to satisfy the boundary condition at the FPC edges. There the boundary condition is obtained by destructive interference between propagating and evanescent modes. Inside the cavity the evanescent mode is not present anymore, and the absence of destructive interference leaves one mode with giant field, as explained in details in [10,11]. The LDOS enhancement up to two orders of magnitude is considered a remarkable property that indeed relates to the giant amplification regimes, as described next. As shown in [25] the Wigner time τ_w is proportional to the spatial average of LDOS over the length of the cavity $\langle \rho(z) \rangle_L$, where the brackets denote a spatial average over the length L . In other words, we may write $\tau_w = K \langle \rho(z) \rangle_L$ where K is a constant, that is a function of the dielectric contrast of the layers [24]. (Note that a concrete analysis of this equivalence along with finding an exact expression of the constant K is outside the scope of this paper, however it can be fully developed following the same procedure detailed in [24]). Therefore, the effective gain coefficient g_{eff} in (1) is in turn proportional to the average of the LDOS and we can also write the gain coefficient enhancement factor as the ratio between LDOS to that in free space

$$g_{\text{eff}} = g_0 \frac{c\tau_w}{L} = g_0 \frac{\langle \rho(z) \rangle_L}{\rho_{\text{free space}}} K, \quad (3)$$

where $\rho_{\text{free space}} = 1/c$, and in our case we find that $K=0.045$. Accordingly, we compare the total power transmission gain G calculated in Fig. 1 at the DBE resonance, and the one estimated by either (1) or (3)

as $G_{\text{approx}} = |T|^2 e^{g_{\text{eff}}}$. The total transmission gain G calculated at the DBE resonance in Fig. 1 at its peak is $G \cong 2 \times 10^4$, while using the approximate formula leads to a peak $G_{\text{approx}} \cong 2.015 \times 10^4$ (here we used $g_0 = 0.11$ based on the value of $n'' = -2.2 \times 10^{-4}$ resulting in $g_{\text{eff}} \cong 10.7$.) This indicates an evident agreement between the exact gain and the estimation using the LDOS or Wigner time, and proves that gain enhancement is intimately related to the boost in Wigner time and LDOS.

Finally, we investigate the gigantic scaling of gain, Wigner time and LDOS with the cavity length. First of all, increasing the number of unit cells, or equivalently the cavity size L , will increase the effective gain coefficient (and hence the total power gain G), quality factor, and LDOS for an FPC. However, for a uniform cavity those parameters can be easily determined analytically, where, for instance, we can determine that the quality factor is linearly proportional to the length of the FPC. For an FPC with RBE, the Wigner time and LDOS are varying as N^2 as calculated using asymptotic analysis [3], and Q -factor as N^3 . Here we show for the first time that an FPC with DBE can enhance the total transmission gain G up to N^5 for values of N ranging from a few up to $N = 90$, and Wigner time and LDOS scale as N^4 , which is a clear and superior enhancement compared to cavities based on the RBE. These trends are determined numerically in Fig. 5(d-f) since the analytical expression has not been developed yet for a photonic crystal with a DBE. Moreover, based on these observations, it can be inferred that a FPC with DBE with smaller length can suffice to achieve even higher gain G of a much larger FPC with RBE.

VI. CONCLUSION AND REMARKS

We have shown that a degenerate band edge (DBE) condition pertaining to an anisotropic stacks of dielectric layers can be utilized to enhance the gain in

Fabry-Perot cavities. We have demonstrated that due to the extremely large Wigner time and the very high local density of states for DBE structures there is consequent giant amplification which is of orders of magnitude larger than the same obtained for uniform cavities or FPCs with RBE. We have also found an optimum condition for the amount of intrinsic active material that maximizes the amplification. One example of a potential application for extremely high gain is provided by Erbium doped fiber amplifiers (EDFA). High Q -factor and giant gain scaling offered by DBE structures can be utilized also in Q -switching and mode locking lasers. For instance, by varying the misalignment angles of the anisotropic layers [36], the dispersion diagram of the periodic structure can be readily altered and hence the Q factor and gain can be significantly switched [37]. These mechanisms have potential in pulsed laser applications and pulse compression optical components. DBE-based giant gain enhancement can find applications in enhancing the amplification in microwave traveling wave tubes (TWT). Indeed, our preliminary results indicate that interaction of a very low energy electron beam with waves in corrugated waveguide with DBE results in extremely high amplifications. Analogous mechanisms can also be used in backward-wave-oscillator sources. In addition to that, radio frequency and microwave solid state distributed amplifiers can also benefit from using active components distributed along a transmission line exhibiting the DBE.

ACKNOWLEDGEMENT

This research was supported by AFOSR MURI Grant FA9550-12-1-0489 administered through the University of New Mexico.

APPENDIX A: TRANSFER MATRICES OF ANISOTROPIC LAYERS

Plane wave propagation along the z direction in a dielectric described by a permittivity tensor follows the simple relation derived from Maxwell equations

$$\frac{\partial}{\partial z} \Psi(z) = ik_0 \underline{\mathbf{M}}(z) \Psi(z), \quad (\text{A1})$$

where $\underline{\mathbf{M}}(z)$ is a matrix operator [10] and $\Psi(z)$ is the state-vector as in Sec. III. In the case where the dielectric is described by a symmetric relative permittivity tensor in the Cartesian coordinates reference as [10,11]

$$\underline{\boldsymbol{\varepsilon}} = \begin{pmatrix} \varepsilon_{xx} & \varepsilon_{xy} & 0 \\ \varepsilon_{xy} & \varepsilon_{yy} & 0 \\ 0 & 0 & \varepsilon_{zz} \end{pmatrix}, \quad (\text{A2})$$

an expression of the operator $\underline{\mathbf{M}}$ can be found as

$$\underline{\mathbf{M}}(z) = \begin{pmatrix} 0 & 0 & 0 & 1 \\ 0 & 0 & -1 & 0 \\ -\varepsilon_{xy} & -\varepsilon_{yy} & 0 & 0 \\ \varepsilon_{xx} & \varepsilon_{xy} & 0 & 0 \end{pmatrix}. \quad (\text{A3})$$

The transfer matrix described in Sec. III is then constructed from the solution of the Cauchy problem in (A1) with the appropriate boundary conditions. In short, the transfer matrix of relative to an individual layer operator $\underline{\mathbf{M}}_m$ is calculated as $\underline{\mathbf{T}}_m = \exp(i\underline{\mathbf{M}}_m d_m)$ [10]. The anisotropic layers considered in this papers have parameters taken from [11], $\varepsilon_{xx} = 16.31$, $\varepsilon_{yy} = 5.79$ and $\varepsilon_{zz} = 1$, though the physical concepts described in this paper are general. The first anisotropic layer in the unit cell in Fig. 1 has an orientation φ of its optical axes with respect to the reference system and has $\varepsilon_{xy} = 5.26$, whereas the second layer has an orientation $-\varphi$, hence it has $\varepsilon_{xy} = -5.26$; This corresponds to a misalignment between the two adjacent anisotropic layers of 45 degrees in the x - y plane, with $\varphi = 22.5$ degrees. The third layer in the unit cell (made of three layers) used to contained a DBE condition is isotropic with $n^2 = \varepsilon_{xx} = \varepsilon_{yy} = \varepsilon_{zz} = 1$. When we consider the active material that leads to gain in the FPC with DBE, we consider it diluted only in the isotropic layer of each unit cell in Fig. 1. The active isotropic materials is assumed to have a refractive index equal

to $n = n' + in'' = 1 - i2.2 \times 10^{-4}$. The same imaginary part of n is considered in the FPC with RBE and in the uniform FPC, shown in Fig. 1.

APPENDIX B: CALCULATION OF THE DYADIC GREEN'S FUNCTION

We outline here the method used to evaluate the Dyadic Green's function $\underline{\mathbf{G}}(z, z')$ in Cartesian coordinates for an planar electric current source located at an arbitrary point z' in a stack of anisotropic layered media, by generalizing the scheme developed in [3,24,34,35] for isotropic media. We consider waves with wavevector along the z -direction therefore we evaluate only transverse-to- z fields due to planar current sources polarized along the x and y directions. Indeed, a sheet source polarized along the z -direction would produce a vanishing transverse fields with wavevector $\mathbf{k} = k\hat{\mathbf{z}}$ and therefore it would lead to $G_{zz}(z, z) = 0$ [38]. Here we briefly elucidate the technique we have used to construct the Green's functions $G_{xx}(z, z')$ and $G_{yy}(z, z')$ for the FPCs under study (more discussion on the method of the Green's function can be found in many mathematical physics textbooks such as Refs. [39,40]). The dyadic Green's function is conveniently constructed from the fundamental set of solutions of the homogenous 1D wave equation for the electric field with the appropriate boundary conditions [40]. We denote the homogenous solutions for $G_{xx}(z, z')$ by $g_{1x}(z)$ and $g_{2x}(z)$, while for $G_{yy}(z, z')$ by $g_{1y}(z)$ and $g_{2y}(z)$. Each solution is a linear combination of exponential functions representing plane waves propagation in the positive or negative z direction inside each layer. We stress that plane waves excited by a source in an FPC made by anisotropic layers are polarization dependent since the x and y polarizations are coupled. Let us now focus on the evaluation of $G_{xx}(z, z')$, then the procedure is analogous for $G_{yy}(z, z')$. As a preliminary example, in free space we have $g_{1x}(z) = e^{ik_0z}$ and $g_{2x}(z) = e^{-ik_0z}$ corresponding to two plane waves propagating in the opposite

directions. In general we use the notation that $g_{1x}(z)$ represents solutions that are excited by an incoming plane wave propagating in the positive z -direction and impinging the cavity from the left (Fig. 1), while $g_{2x}(z)$ represents solutions that are excited by an incoming plane wave propagating the negative z -direction [24,34,35]. For the layered anisotropic media surrounded by vacuum (Fig. 1), we obtain $g_{1x}(z)$ and $g_{2x}(z)$ using the transfer matrix approach developed in Appendix A, utilizing the knowledge of the transfer matrix of the individual layers, considering the two external excitations. As a result, the solutions satisfy boundary conditions at all interfaces as well as the outgoing waves condition [24,34,35] outside the cavity (in the $\pm z$ direction). Following the procedure in [24,40], we can write $G_{xx}(z, z')$ as

$$G_{xx}(z, z') = \begin{cases} f_{1x}(z')g_{1x}(z), & 0 \leq z < z' \\ f_{2x}(z')g_{2x}(z), & z' < z \leq L \end{cases}, \quad (\text{B1})$$

where $f_{1x}(z')$ and $f_{2x}(z')$ are functions of the source location z' . We then enforce the continuity of $G_{xx}(z, z')$ as well as resolve the jump discontinuity of its first derivative due to a Dirac delta source, at $z = z'$ [40]. This allows us to express $f_1(z')$ and $f_2(z')$ using the Wronskian [40]. After some mathematical manipulation (similar to the steps in [24,34,40]) we obtain an expression for $G_{xx}(z, z)$, i.e., for $z = z'$, that reads

$$G_{xx}(z, z) = \frac{g_{1x}(z)g_{2x}(z)}{2ik_0T_{xx}}. \quad (\text{B2})$$

Here T_{xx} is the transmission coefficient also defined as the normalized inner product $T_{xx} = \langle \mathbf{E}_x^i, \mathbf{E}^t \rangle / \|\mathbf{E}_x^i\|$, where \mathbf{E}_x^i is an x -polarized incident electric field vector from the vacuum region and \mathbf{E}^t is the transmitted electric field vector, and we have used the time reversal symmetry property that the transmission

coefficient of the structure excited from vacuum in either the $+z$ or $-z$ directions (i.e., transmission through the FPC from left to right or from right to left, Fig. 1) is the same [24,34]. Analogously we can obtain $G_{yy}(z, z)$ following the same steps. The LDOS in (2) is proportional to the trace of the imaginary part of the dyadic Green's function, i.e.,

$$\rho(z) = -2 \frac{k_0}{\pi c} \left(\text{Im} \left(G_{xx}(z, z) + G_{yy}(z, z) \right) \right).$$

REFERENCES

- [1] K. Inoue, M. Sasada, J. Kawamata, K. Sakoda, and J. W. Haus, *Jpn. J. Appl. Phys.* **38**, L157 (1999).
- [2] H.-Y. Ryu, S.-H. Kwon, Y.-J. Lee, Y.-H. Lee, and J.-S. Kim, *Appl. Phys. Lett.* **80**, 3476 (2002).
- [3] J. M. Bendickson, J. P. Dowling, and M. Scalora, *Phys. Rev. E* **53**, 4107 (1996).
- [4] B.-S. Song, S. Noda, T. Asano, and Y. Akahane, *Nat. Mater.* **4**, 207 (2005).
- [5] B. Maune, M. Lončar, J. Witzens, M. Hochberg, T. Baehr-Jones, D. Psaltis, A. Scherer, and Y. Qiu, *Appl. Phys. Lett.* **85**, 360 (2004).
- [6] S. John and J. Wang, *Phys. Rev. B* **43**, 12772 (1991).
- [7] N. V. Bloch, K. Shemer, A. Shapira, R. Shiloh, I. Juwiler, and A. Arie, *Phys. Rev. Lett.* **108**, 233902 (2012).
- [8] I. Bayn, B. Meyler, A. Lahav, J. Salzman, R. Kalish, B. A. Fairchild, S. Praver, M. Barth, O. Benson, and T. Wolf, *Diam. Relat. Mater.* **20**, 937 (2011).
- [9] A. Figotin and I. Vitebskiy, *Phys. Rev. E* **68**, 036609 (2003).
- [10] A. Figotin and I. Vitebskiy, *Phys. Rev. E* **72**, 036619 (2005).
- [11] A. Figotin and I. Vitebskiy, *Phys. Rev. E* **74**, 066613 (2006).
- [12] A. Figotin and I. Vitebskiy, *Phys. Rev. A* **76**, 053839 (2007).
- [13] A. Figotin and I. Vitebskiy, *Laser Photonics Rev.* **5**, 201 (2011).
- [14] P. Yeh and C. Gu, *Optics of Liquid Crystal Displays* (John Wiley & Sons, 2010).
- [15] J. R. Burr, N. Gutman, C. Martijn de Sterke, I. Vitebskiy, and R. M. Reano, *Opt. Express* **21**, 8736 (2013).
- [16] N. Gutman, C. Martijn de Sterke, A. A. Sukhorukov, and L. C. Botten, *Phys. Rev. A* **85**, (2012).
- [17] N. Gutman, W. H. Dupree, Y. Sun, A. A. Sukhorukov, and C. M. de Sterke, *Opt. Express* **20**, 3519 (2012).
- [18] R. Colombelli, K. Srinivasan, M. Troccoli, O. Painter, C. F. Gmachl, D. M. Tennant, A. M. Sergent, D. L. Sivco, A. Y. Cho, and F. Capasso, *Science* **302**, 1374 (2003).
- [19] A. Figotin and I. Vitebskiy, ArXiv09091393 *Phys.* (2009).
- [20] J. P. Dowling, M. Scalora, M. J. Bloemer, and C. M. Bowden, *J. Appl. Phys.* **75**, 1896 (1994).
- [21] J. Grgić, J. R. Ott, F. Wang, O. Sigmund, A.-P. Jauho, J. Mørk, and N. A. Mortensen, *Phys. Rev. Lett.* **108**, 183903 (2012).
- [22] H. Noh, J.-K. Yang, I. Vitebskiy, A. Figotin, and H. Cao, *Phys. Rev. A* **82**, 013801 (2010).
- [23] M. Fox, *Quantum Optics: An Introduction: An Introduction* (Oxford University Press, 2006).
- [24] G. D'Aguanno, N. Mattiucci, M. Scalora, M. J. Bloemer, and A. M. Zheltikov, *Phys. Rev. E* **70**, 016612 (2004).
- [25] J. T. Verdeyen, *Laser Electron. Ed. JT Verdeyen* Englewood Cliffs NJ Prentice Hall 1989 640 P **1**, (1989).
- [26] Y. Amnon, *Quantum Electronics*, 3rd Edition (Wiley, 1989).
- [27] A. Yariv and P. Yeh, *Photonics: Optical Electronics in Modern Communications (The Oxford Series in Electrical and Computer Engineering)* (Oxford University Press, Inc., 2006).
- [28] F. T. Smith, *Phys. Rev.* **118**, 349 (1960).
- [29] G. L. Matthaei, L. Young, and E. M. Jones, *DESIGN OF MICROWAVE FILTERS, IMPEDANCE-MATCHING NETWORKS, AND COUPLING STRUCTURES. VOLUME 2* (DTIC Document, 1963).
- [30] H. G. Winful, *New J. Phys.* **8**, 101 (2006).
- [31] T. Lauprêtre, C. Proux, R. Ghosh, S. Schwartz, F. Goldfarb, and F. Bretenaker, *Opt. Lett.* **36**, 1551 (2011).
- [32] H.-Y. Yao, N.-C. Chen, T.-H. Chang, and H. G. Winful, *Phys. Rev. A* **86**, 053832 (2012).
- [33] P. Sheng, *Introduction to Wave Scattering, Localization and Mesoscopic Phenomena: Localization and Mesoscopic Phenomena* (Springer, 2006).
- [34] O. D. Stefano, S. Savasta, and R. Girlanda, *J. Mod. Opt.* **48**, 67 (2001).
- [35] G. D'Aguanno, M. Centini, M. Scalora, C. Sibilìa, M. Bertolotti, M. J. Bloemer, and C. M. Bowden, *JOSA B* **19**, 2111 (2002).
- [36] K.-Y. Jung and F. L. Teixeira, *Phys. Rev. B* **77**, 125108 (2008).
- [37] V. A. Tamma, A. Figotin, and F. Capolino, ArXiv13107645 *Phys.* (2013).
- [38] N. Marcuvitz and J. Schwinger, *J. Appl. Phys.* **22**, 806 (1951).
- [39] B. Friedman, *Principles and Techniques of Applied Mathematics* (New York, 1961).
- [40] P. Dennery and A. Krzywicki, *Mathematics for Physicists* (Courier Dover Publications, 1996).